Polypyrrole/MnO_2 nanocomposites as potential electrodes for supercapacitor

Ritu P. Mahore[1*], Devendra K. Burghate[1], Subhash B. Kondawar[2], Ashish P.Mahajan[2], Deoram V. Nandanwar[3]

[1]*Department of Physics, Shri Shivaji Science College, Nagpur 440012, India*
[2]*Department of Physics, Rashtrasant Tukadoji Maharaj Nagpur University, Nagpur 440033, India*
[3]*Department of Physics, Mathuradas Mohata College of Science, Nagpur 440023, India*

*Corresponding author

DOI: 10.5185/amlett.2018.1573
www.vbripress.com/aml

Abstract

Due to the ever growing demand of energy for various applications attention of researchers is aroused by Supercapacitors due to its superior power, energy density and cyclic life. Electrode material mainly determines the performance of Supercapacitors. Conducting polymers, metal oxides and carbon based materials are mainly used as electrode materials in Supercapacitors. Among these three categories of materials, Conducting polymers and metal oxides shows pseudo-capacitance. This paper reported the synthesis of Pure Polypyrrole (PPy) and Polypyrrole/Manganese dioxide (PPy/MnO_2) nanocomposites by in-situ chemical oxidative polymerization. The synthesized materials were tested as potential candidates for the electrodes of supercapacitor. X-ray diffraction (XRD), Fourier transform infrared spectroscopy (FTIR), Scanning electron microscopy (SEM) revealed that nanoparticles of MnO_2 are well incorporated into PPy matrix. Cyclic Voltammetry (CV) indicated that PPy/MnO_2 nanocomposites have an ideal capacitive behaviour and an excellent cyclibility. Electrochemical impedance spectroscopy (EIS) and Galvanostatic charge-discharge (GCD) measurements proved that nanocomposite electrode with 10% MnO_2 composition showed the smallest charge transfer resistance and highest specific capacitance compared to other compositions. The electrochemical studies of PPy/MnO_2 nanocomposites showed that PPy/MnO_2 nanocomposites are suitable advanced materials for electrodes of the supercapacitors.

Keywords: Polypyrrole, manganese dioxide, nanocomposites, supercapacitor.

Introduction

Humanity is demanding a large quantity of energy as its level of development is growing, coupled with the severe climate change. The need of electronic portable equipment, wireless sensor networks and other micro systems are responsible for increasing demand for better energy storage and power supply under various conditions. Power devices integrated with other elements can fulfill the desire to further miniaturize existing on-chip systems. Energy storage becomes a critical factor that can solve the problems described above. The development of energy storage devices is extremely important to store the harvested energy for wide applications, thus it is gaining extensive research interest due to growing world population, global climate change, concerns about exhaustion of fossil fuels **[1, 2].**

Fuel cell, batteries, Supercapacitors, and conventional capacitors are the major energy storage and conversion devices. Amongst these devices supercapacitor is most efficient energy storage device due to their simple fabrication method greater power density, long cycle life **[3].** Supercapacitors also known as electrochemical capacitors have attracted much attention due to fast charging and discharging within seconds, superior cycle life time, high reliability and high power density. Supercapacitors, based on their charge storage mechanism can be broadly classified into two catogories: electrical double layer capacitors (EDLCs) and pseudo-capacitors. Energy storage in an EDLC is due to the charging of the electrical double layer at electrode and electrolyte interface while a pseudo-capacitor utilizes faradic reactions in addition to double layer charge. A conducting electro-active electrode with large surface area accessible to the electrolytic dopant ions is major factor responsible for high performance Supercapacitors **[4].** Conducting polymers, carbon-based materials and transition-metal oxides have been investigated to explore the great potential and applicability for advanced supercapacitors with high capacity performance. However, from earlier attempts it can be concluded that the electrochemical properties of indivudual material separately for supercapacitors were limited by their intrinsic structural shortcomings. For example, carbon nanotubes (CNTs) exhibits high conductivity, good mechanical properties,large surface area and chemical stability **[5,**

6], CNT-based electrodes act only as a stable high-surface-area support without redox properties, hence resulting in relative low specific capacitance **[7-9].** Conducting polymers have huge capacity loss during successive charge/discharge cycles restricts their application for supercapacitors. In addition to this MnO_2 is an important member of transition-metal oxides which is regarded as one of the most promising pseudocapacitive materials because of its low cost, high specific capacitance, environmental friendliness and natural abundance **[10, 11].** However, the electrochemical performances of MnO_2 are basically limited by dense morphology of the oxide and poor electronic conductivity **[12, 13].** Hence, considerable research efforts have been placed on exploring hybrid composite structures where MnO_2 is combined with highly conductive materials such as metal nanostructures, carbon nanotubes (CNTs), graphene or conducting polymers ((e.g. polypyrrole (PPy), polythiophene(PTh),poly(3,4- ethylene dioxyt hiophene) (PEDOT) and polyaniline (PANI) to improve the electrical conductivity of MnO_2-based electrodes for optimized electrochemical performance. **[14, 15].**

To improve the conductivity of MnO_2 and cyclic life of conducting polymer Polypyrrole (PPy), we have synthesized pure conducting polypyrrole (PPy) and PPy/ MnO_2 nanocomposites with 5, 10 and 15weight % of MnO_2 (PM5, PM10 and PM15) by using an in-situ chemical oxidative method for the study of electrochemical performance to find the synergistic effect of both the components suitable for supercapacitors. The electrochemical performance of PPy/MnO_2 nanocomposites is systematically compared with that of pure polypyrrole using Cyclic Voltammetry(CV) , Galvanostatic Charge-Discharge (GCD), Electrochemical Impedance Spectroscopy (EIS) and their structural characterizations using XRD, FTIR spectral analysis and SEM.

Experimental

Materials/ Chemicals details

The monomer pyrrole (99%) was purchased from Sigma-Aldrich and purified prior to use and stored below 5ºC. All other reagents including $FeCl_3$ (purity 99.5%) as oxidant, $K_2Cr_2O_7$/$KMnO_4$, $MnCl_2{\cdot}4H_2O$ precursors for MnO_2 were procured from Sigma–Aldrich and used as received without further purification. All other chemicals were of AR grade used for the synthesis. Solutions were prepared in de-ionized water.

Synthesis of *MnO_2 nanostructure*

$KMnO_4$ and $K_2Cr_2O_7$ in molar ratio of $K_2Cr_2O_7$/$KMnO_4$ (0.25:0.1) were dissolved in 150 mL de-ionized water and mixed drop wise into the $MnCl_2$ solution under constant stirring. The brown color suspension was then heated and refluxed. The black solid product was filtered and washed using de-ionized water to obtain nanostructure MnO_2 **[16].**

Synthesis of Polypyrrole and Polypyrrole/MnO_2 Nanocomposites

500µL pyrrole was slowly added to 50 mL anhydrous ferric chloride (1.94 g $FeCl_3$) solution and the polymerization was allowed to continue for 4 h with constant stirring. The precipitate was filtered, washed thoroughly using de-ionized water and then dried to get polypyrrole (PPy). PPy/MnO_2 nanocomposite was synthesized by an *in-situ* chemical oxidation polymerization. In a typical reaction, 5% MnO_2 (by weight of PPy) was mixed to 50 mL anhydrous ferric chloride (1.94 g $FeCl_3$) solution. 500µL pyrrole was slowly added drop wise and the polymerization was allowed to continue for 4 h with constant stirring. The precipitated composite was filtered, washed thoroughly with de-ionized water and then dried to get PPy/MnO_2 nanocomposite **[17].** The similar procedure was carried out for 10% and 15% MnO_2.

Characterizations

X-ray powder diffraction pattern of nanostructure samples were recorded on Regaku Mini-Flex II a bench top X-ray diffraction instrument which uses Cu-Kα radiation of wavelength 0.15418 Å for characterization of continuous scan of 5º/min. with an accuracy of 0.02 at 30 KV and 15 mA. Bruker Alpha model was used to obtain FTIR spectra. Scanning Electron Microscope SEM-JEOL-6390LV with the magnification of 300000X was used to study the surface morphology. Electrochemical studies were done using electrochemical analyser (CH Model 600D series). Electrochemical Impedance spectroscopy (EIS) technique was carried out on Interface 1000 Gamry Potentiostat.

Results and discussion

X-ray diffraction

The XRD patterns of Pure PPy, Pure MnO_2 and PPy/ MnO_2 (PM10) nanocomposite are shown in **Fig. 1(a), (b) and (c)** respectively. XRD pattern of PPy exhibits a broad characteristic peak at 2θ = 25° broad characteristic peak at about 25° of pure PPy exhibits that pure PPy is amorphous., implying an amorphous structure **[18,19].** XRD patterns of MnO_2 the diffraction peaks at 2θ = 28.81°, 37.41°, 49.81° and 60.21° indicates the presence of pure tetragonal phase of α-MnO2 (JCPDS 44-0141).Strong diffraction peaks are observed which are responsible for good crystalline nature other characteristic impurity peaks are not observed, resulting in high purity of α-MnO_2 **[20, 21].** In XRD pattern of PPy/MnO_2, broad characteristic of PPy is seen at 2θ= 26° and the peaks of MnO_2 are also seen in the XRD pattern of composite thus it can be concluded that there is presence of MnO_2 in composite.

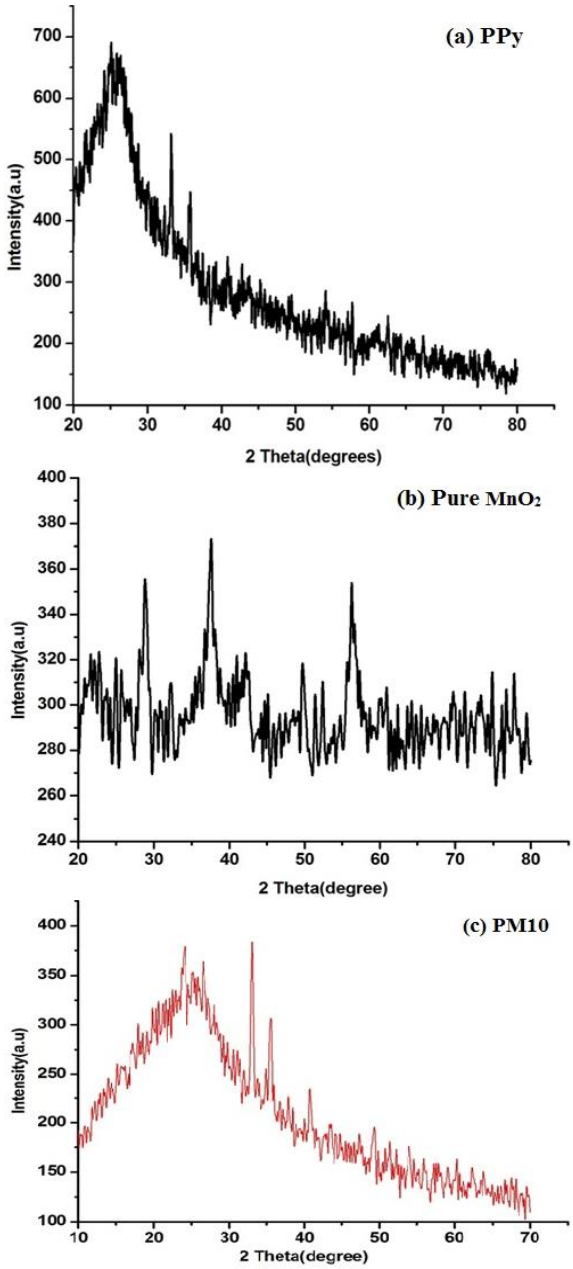

Fig. 1. XRD patterns of (a)Pure PPy,(b) Pure MnO_2 and (c) PM10.

Fourier Transform Infrared Spectroscopy

FTIR spectra of PPy and PPy/MnO_2 nanocomposites are shown in **Fig 2.** FTIR spectrum of pure PPy shows that the absorption bands at 1535 and 1454cm^{-1} are associated with the C–C and C–N stretching of the pyrrole ring. The band at 2923cm^{-1} and 2853cm^{-1} refers to C-H stretching vibration. Transmittance peak at 1171cm^{-1} was assigned to N–C stretching. The peaks at 1307 and 1047cm^{-1} are ascribed to in-plain C–H deformation and in-plain N–H stretching vibrations, respectively. The conducting state of PPy can be concluded from strong peaks observed at 1172 and 913cm^{-1}**[22, 23].** FTIR spectra of the prepared PPy/MnO_2 nanocomposites shows the existence of pure MnO_2, three distinct adsorption peaks at 716cm^{-1}, 520cm^{-1} and 465cm^{-1} can be attributed to the Mn-O stretching vibrations. The existence of bands at 1550, 1304, 1160, 1044 and 780cm^{-1} indicates the formation of PPy in nanocomposites. FTIR spectra of PPy and PPy/MnO_2 composite when observed carefully, it can be seen that the intensity and position intensity of PPy peaks were influenced by incorporation of MnO_2 in the PPy/MnO_2 composite, although the two spectra of PPy/MnO_2 composite and PPy are very similar. It is worthy to note that the C-N stretching vibration at 1169cm^{-1} and the C-H out-of-plane vibration at 964cm^{-1} are induced by doping anions, revealing PPy is in doping state. In addition, the C = O stretching vibrations related to carbonyl/carboxyl groups can be observed around 1708cm^{-1}, indicating the interfacial interaction between PPy and MnO_2 **[24, 25].**

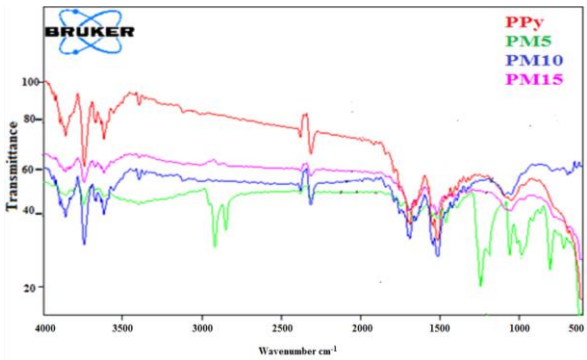

Fig. 2. FTIR spectra of Pure PPy and PPy/MnO_2 nanocomposites.

Scanning electron microscopy

Fig. 3 (a), (b), (c), (d) and **(e)** exhibits the SEM images of MnO_2, PPy, PM5, PM10 and PM15 respectively. SEM image of pure MnO_2 indicates that particles of MnO_2 are mainly composed of small spherical granular particles whose diameters are in nanoscale. The smaller particles have larger specific surface area and shorter diffusion distance, which can provide faster probability, higher material utilization, and better rate performance in active materials. The polymerization was initiated at the interface between the two immiscible liquids leads to formation of irregular sphere like structure which can be found in SEM image of PPy **[26, 27].** Morphologically PPy shows the existence of small globules with relatively small primary particle size in the range of 30nm - 50 nm and porous surface which can be beneficial for ion diffusion **[28]**. PPy/MnO_2 nanocomposites morphology clearly exhibits large surface area of the co-deposited MnO_2. The porosity of PPy provides a large surface to the growing MnO_2 providing a high active surface area of the MnO_2 particles. An ordered and shorter structure of PPy polymer is considered to be an ideal structure for charge storage. The presence of MnO_2 in PPy scaffold leads to cross linking the PPy chains which in turn enhances the conductivity of composite. The pseudocapacitance of MnO_2 significantly relies on the surface atoms and in case of PPy/MnO_2 nanocomposite, the available large surface of supported MnO_2

nanoparticles significantly contribute to the overall capacitance. Therefore, the large surface area of the embedded MnO_2 nanoparticles as well as structurally modified PPy polymer chains due to MnO_2 nucleation both contribute to the high specific capacitance of the nanocomposites **[29].**

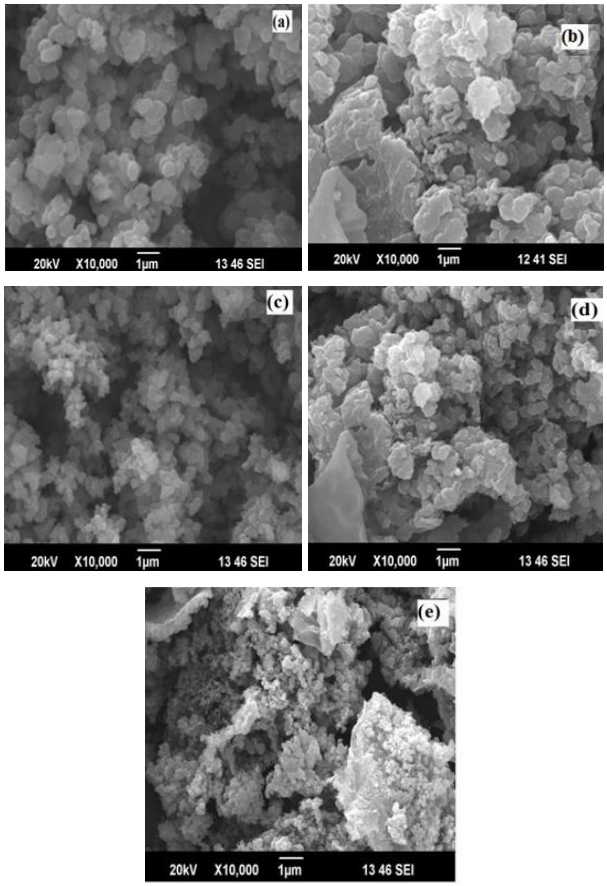

Fig. 3. SEM images of (a) Pure MnO2,(b) Pure PPy (c) PM5, (d) PM10 and (e) PM15

Electrochemical performance

Fig. 4. illustrates cyclic voltammograms of PPy and PPy/MnO_2 at the scan rate of 50mV/s. Cyclic voltammetric scanning was performed in an aqueous solution of 1M Na_2SO_4 with a potential window -1.0 to +0.6V versus Ag /AgCl . The area under CV curve divided by scan rate gives the value of capacitance. From the CV curves it can be seen that the there is slight change in area of CV of PM10 indicating high capacitive value. Thus it can be said that PPy/MnO_2 electrodes with 10% MnO_2 show high capacitance. The quasi-rectangular profile is well-maintained in all the composites, indicating good rate capability. It is interesting to note that both MnO_2 and PPy components can contribute remarkable pseudocapacitance to the overall capacitance of the composites **[30].** Capacitance behaviours and cyclic life of as prepared samples of PPy, PM5, PM10 and PM15 were studied by galvanostatic charge–discharge cycling. **Fig. 5** illustrates the Galvanostatic Charge-Discharge (GCD) curves of PPy/MnO_2 nnaocomposites at the current density of 2 A/g. Galvanostatic Charge–Discharge experiments were performed from -0.05 to 0.45V. The specific capacitance of electrodes was estimated from the discharge curves **[31].**

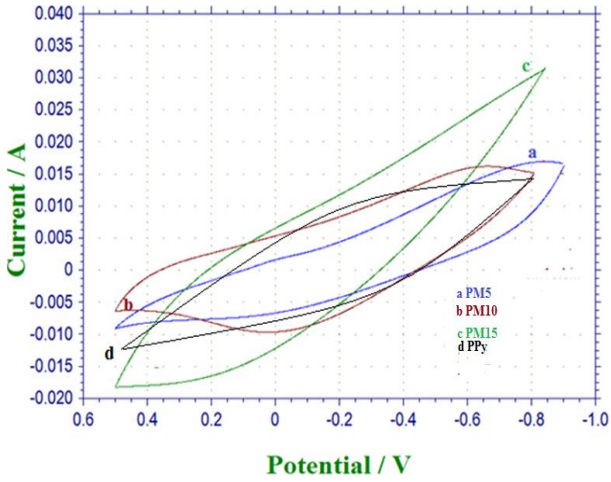

Fig. 4. Cyclic Voltammograms of PPy/MnO_2 composites at scan rate 50mV/s.

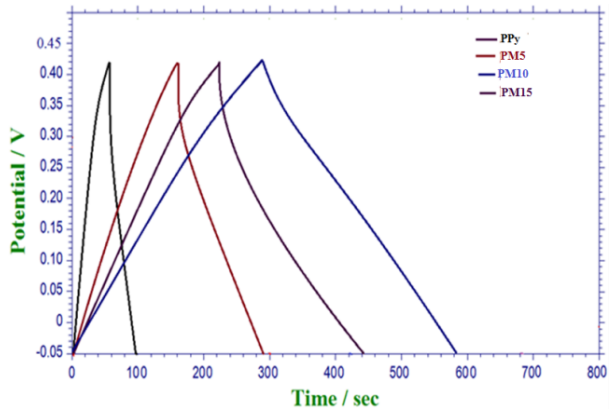

Fig. 5. Galvanostatic Charge-Discharge of PPy/MnO_2.

The specific capacitance of PPy, PM5, PM10 and PM15 was found to 208, 329, 385 and 365 F/g respectively. The GCD curves approximately have equal charging and discharging periods, implying a favourable electrochemical reversibility. When the current density lowers, the non-straight sections in GCD curves become more obvious, indicating a high faradaic contribution to the charge accumulation process. However, the charge/discharge curves of PPy and PPy composite with MnO_2 exhibits a capacitive behavior with almost symmetric charge/discharge plots with a deviation to the linearity, revealing the synergistic contribution among pseudocapacitive behavior of MnO_2 and PPy. The linear voltage versus time profiles and the quick I–V response suggest that the MnO_2 are good electrode materials for Supercapacitors. Among the charge/discharge curves of polypyrrole/ MnO_2 with 5, 10 and 15 weight % of MnO_2 (PM5, PM 10 and PM15 resp.) it can be seen that the time required for charge-discharge is more for Polypyrrole/ MnO_2 with 10% **[32, 33].**

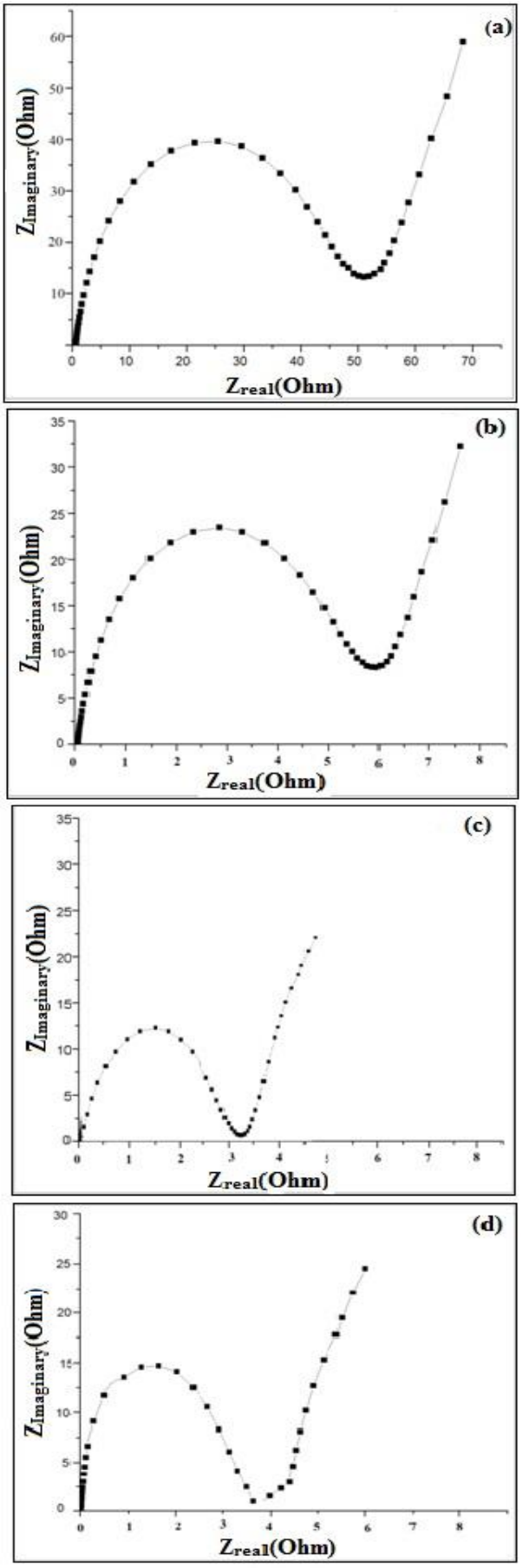

Fig. 6. Nyquist plot for (a) PPy, (b) PM5, (c) PM10 and (d) PM15.

EIS was carried out in three-electrode system in 1M Na_2SO_4 as an electrolyte. Nyquist plot gives the resistive and capacitive behavior of any material. In Nyquist plot, the real axis intercept represents the equivalent series resistance (ESR), including the contact resistance and the intrinsic resistance of the active materials and the electrolyte. Smaller ESR values imply the higher conductivity, smaller diameter of the semicircle in represents the lower charge transfer resistance and the vertical line in a low frequency range, indicates the nearly ideal capacitive behaviours. **Fig. 6(a), (b), (C)** and **(d)** presents the resulting Nyquist plots for PPy PM5, PM10 and PM15 respectively. All figures, clearly shows the small semicircle (first portion), Warburg diffusion line (second portion) and capacitive line (third portion). A relatively small semicircle in the high frequency region represents the dominant resistive nature of the electrochemical cell consisting of electrode/electrolyte/current-collector. The beginning of the semicircle line (left-intercept of Z_{imag} at the Z_{real} axis) represents the resistance (Rs) of the electrolyte in contact with the current collector and electrode. The termination of the semicircle line (right-intercept of Z_{imag} at the Z_{real} axis) represents the internal resistance (Rp) of the electrode. The diameter of the semicircle (Rp-Rs) is equal to the ESR value. The ESR value from the Nyquist plot for PPy, PM5, PM10 and PM15 are 49.95, 5.7, 3.15 and 3.55. The linear slopes with a large phase angle manifest that these electrodes exhibit almost purely capacitive behavior at low frequencies. The compressed semicircle at high frequencies represents a typical resistive behavior These results demonstrate the PPy/ MnO_2 composites hold a particular promise as electrode materials for Supercapacitor **[34].**

Conclusion

Polypyrrole/MnO_2 with different weight percentage (PM5, PM10, PM15) have been successfully synthesized by in-situ chemical oxidative polymerization method. Polypyrrole/Manganese dioxide (PPy/MnO_2) nanocomposites showed excellent increase in specific capacitance as potential candidates for the electrodes of supercapacitor. 10% MnO_2 composition in all as-synthesized PPy/MnO_2 nanocomposites showed the smallest charge transfer resistance and highest specific capacitance compared to other compositions.

Acknowledgements

The present work was supported by University Grant Commission (UGC), NewDelhi, India under Major Research Project (F.No 41-931/2012). The authors are thankful to UGC for financial support to carry out this work**.**

Author's contributions

Conceived the plan: RPM, DKB, SBK; Performed the expeirments: RPM, APM; Data analysis: SBK, RPM, APM, DVN; Wrote the paper: RPM, SBK. Authors have no competing financial interests.

Supporting information

Supporting informations are available from VBRI Press.

References

1. Li, S.; Wang, Y.; Yang, S; Liu, C.; Chang, K.; Tien, H.; Wen, P; Maa, C.; Hu, C.; *Journal of Power Sources*, **2013,** *225*, 347. **DOI:**10.1016/j.jpowsour.2012.10.037
2. Chen, Z.; Wei, C.; Gong, Y.; Lv, J.; Du, R.; *Int. J. Electrochem. Sci.*, **2016**, 11, 9800-9811. **DOI:** 10.20964/2016.12.67
3. Sankar, K.; Selvan, R.; *J. Power Sources*, **2015**, *275*, 399. **DOI:** 10.1016/j.jpowsour.2015.10.183
4. Sharma, R.; Zhai, L.; *Electrochimica Acta*, **2009**, *54*, 7148. **DOI:** 10.1016/j.electacta.2009.07.048
5. Hu, L.; Pasta, M.; Mantia, F.L.; Cui, L.; Jeong, S.; Deshazer, H .D.; Choi, J.W.; Han, S.M.; Cui,Y.; *Nano Lett.*, **2010**,*10*,708. **DOI:** 10.1021/nl903949m
6. Largeot, C.; Portet, C.; Chmiola, J.; Taberna, P.L.; Gogotsi, Y.; Simon, P.; *J. Am. Chem. Soc.*,**2008**, *130*, 2730. **DOI:** 10.1021/ja7106178
7. Zheng, H.J.; Kang, W.; Zhao, F.M.; Tang, F.Q.; Rufford, T.E.; Wang, L.Z.; Ma, C.N; *Solid State Ionics*, **2010**, *181* 1690. **DOI:** 10.1016/j.jpowsour.2012.06.047
8. Lee, S. W.; Kim, J.; Chen,S.; Hammond, P.T.; Yang, S,H.; *ACS Nano*, **2010**, 3889. **DOI:** 10.1039/C5NJ00348B
9. Wu, Z.S.; Ren,W.; Wang, D.W.; Li, F.; Liu, B.; Cheng, H.M.; *ACS Nano*, **2010**, *4*, 5835. **DOI:** 10.1021/nn101754k
10. Chen, S.; Zhu, J.; Wu, X.; Han, Q.; Wang, X.; *ACS Nano*, **2010**, *4*, 2822. **DOI:** 10.1021/nn901311t.
11. De Yan, D.; Liu, Y.; Wu, Z.; Zhuo, R.; Wang, J.; *Advanced Materials Research*, **2013**, *800*, 393-397. **DOI:** 10.4028/www.scientific.net/AMR.800.393
12. Sonia, G.; Shekhar, S.; Sharma, R.; Singh, G.; *Electrochimica Acta* , **2014**, *116*, 137. **DOI:** 10.1016/j.electacta.2013.10.173
13. Peng. L.; Feng, Y.; Li, Y.; Feng, W.; *Journal of Power Sources*, **2012**, *220*,160. **DOI:** 10.1016/j.jpowsour.2012.07.073
14. Chena, J.; Wanga, Y Caoa, J.; Liu, Y.; Ouyanga, J.; Jiaa, D.; Zhoua, Y.; *Electrochimica Acta*, **2015**, *182*, 861–870 **DOI:** 10.1016/j.electacta.2015.10.015
15. Yu, G.; Hu, L.; Liu, N.; Wang, H.; Vosgueritchian, M.; Yang, Y.; Cui, Y.; Bao, Z.; *Nano Lett.* **2011**, *11*, 4438. **DOI:** 10.1021/nl2026635
16. Chen, L.; Song, Z.; Liu, G.; Qiu, J.; Yu, C.; Qin, J.; Ma, L.; Tian, T.; Liu, W.; *Journal of Physics and Chemistry of Solids*, **2013**, *74*, 360. **DOI:** 10.1016/j.jpcs.2012.10.013
17. Mahore,R.; Burghate,D.; Kondawar,S.; *Advance Material Letter*, **2014**, *7*, 400. **DOI:** 10.5185/amlett.2014.amwc.1038
18. Wang, B.; Qiu, J.; Feng, H.; Sakai, E.; Electrochimica *Acta*, **2015,** *151*, 230. **DOI:** 10.1016/j.electacta.2014.10.153
19. SuN.; Li, H.; Yuan, S.; Yi, S.; Yin, E.; *EXPRESS Polymer Letters*, **2012**, *6*, 697. **DOI:** 10.3144/expresspolymlett.2012.75
20. Chen, L., Song, Z. ; Qiu, J.; Yu, J. Qin, Ma, L.; Tian, F.; W. Liu, *J. Phys. Chem. Solids*, **2013**, *74*, 360. **DOI:** 10.1016/j.jpcs.2012.10.013
21. Yao, W.; Zhou, H.; Lu, Y.; *Journal of Power Sources*, **2013**, 214, 359. **DOI:** 10.1016/j.jpowsour.2013.04.142
22. Ning, N.; Fu, S.; Zhang, W.; Chen, F.; Wang, K.; Deng, H.; Zhang, Q.; Fu, Q.; *Progress in Polymer Science*, **2012**, *37*, 1425– 1455. **DOI:** 10.1016/j.progpolymsci.2011.12.005
23. Chougulea, M.; Pawara, S.; Godsea, P.; Mulika, R.; Sen, S.; Patila, V.; *Soft Nanoscience Letters*, **2011,** *1***,** 6. **DOI:** 10.4236/snl.2011.11002
24. Wang, J.; Yang, Y.; Huang, Z.; Kang, F.; *Electrochimica Acta;* **2014**, *130*, 642
. **DOI:** 10.1016/j.electacta.2014.03.082
25. Sharma, A. K.; Sharma, Y.; Malhotra, R.; Sharma, J.K. *Adv. Mat. Lett.* **2012**, *3*(2), 82. **DOI:** 10.5185/amlett.2012.1315
26. Bora, C,; Dolui, S.K.; *Polymer ;* **2012**, *53*, 923. **DOI:** 10.1016/j.polymer.2011.12.054
27. Zhang, Y.; Li,G.; Lv, Y.; Wang, L.; Song, Z.; Huang, B,; *International Journal of Hydrogen Energy*; **2011**, 36, 11760. **DOI:** 10.1016/j.ijhydene.2011.06.020
28. Lai, C.; Zhou, Z.; Fong, H.; *Journal of Power Sources*, **2014,** *247*, 134. **DOI:** 10.1016/j.jpowsour.2013.08.082
29. Sharma, R.; Rastogi, A.; Desu, S.; *Electrochimica Acta*, **2008**, *53*, 7690 **DOI:** 10.1016/j.electacta.2008.04.028
30. Zheng, T.; Lu, X.; Bian, X.; Zhang, C.; Xue, Y.; Jia, X.; Wang, C.; *Talanta*, **2012,** *90*, 51. **DOI:** 10.1016/j.talanta.2011.12.066
31. Chen, Y.; Du, L.; Yang, P.; Sun, P.; *Journal of Power Sources*, **2015,** *287* ,68. **DOI:** 10.1016/j.jpowsour.2015.04.026
32. Salasa, I.; Sudhakar, Y.; Selvakumar M.; *Applied Surface Science;* **2014**, 296, 195. **DOI:** 10.1016/j.apsusc.2014.01.080
33. Zhu, Y.; Shi, K.; Zhitomirsky, I; *Journal of Power Sources*, **2014**, *268*, 233. **DOI:** 10.1016/j.jpowsour.2014.06.046
34. Wang, J.; Yang, Y.; Huangc, Z.; Kang, F.; *Electrochimica Acta*, **2014**, *130*, 642. **DOI:** 10.1016/j.electacta.2014.03.082

